PHILIPPINE ENGINEERING JOURNAL
PEJ 2014; Vol. 35, No. 2: 38-56

Short Communications

EJECTOR PROFILE MODELLING FOR COMPRESSOR-DRIVEN EJECTOR REFRIGERATION SYSTEM

John Carlo S. Garcia, Joselito Yam T. Alcaraz, Joseph Reymond T. Alvarez, Binoe E. Abuan, Menandro S. Berana
Department of Mechanical Engineering, College of Engineering,
University of the Philippines, Diliman Quezon City, 1101 Philippines

ABSTRACT

This paper provides a comprehensive description of the design of the ejector dimensions based on the thermodynamic properties of the refrigerant without allowing the ejector to experience shock. A nozzle and a diffuser with converging-diverging sections are used to avoid formation of shock along the mixing section of the ejector. The analysis of the fluid flow within the system is assumed to be homogenous and one-dimensional. The program produced in this paper is used for determining the geometry of the ejector based on the input parameters in the system—evaporating and condensing temperature, evaporator mass flow rate, and entrainment ratio. This paper also presents the performance of different refrigerants used in the compressor-driven refrigeration system with the same input parameters. The program has produced the corresponding ejector profile along with the pressure and velocity across the geometry for a certain set of input parameters. It is also found out that ammonia has the highest coefficient of performance (COP) among the refrigerants used in the study.

Keywords: *Ejector, compressor, refrigeration, COP.*

Correspondence to: Menandro S. Berana, Department of Mechanical Engineering, University of the Philippines, Diliman, Quezon City, 1101 Philippines, Email: menandro.berana@coe.upd.edu.ph

1. INTRODUCTION

One of the emerging technologies in refrigeration is the *ejector-refrigeration system* (ERS). Ejector refrigeration systems are refrigeration systems wherein the use of an ejector is utilized as a compressor or as an expansion device. ERS seems to be more attractive than the traditional vapor compression refrigeration systems because of its simplicity in construction, installation, and maintenance. However, this type of refrigeration system has relatively low COP which made it less dominant in the market than the conventional one. Thus, currently, researchers are engaged in enhancing ERS performance by combining it with other refrigeration cycles or by varying the ejector's function within the cycle to improve the system overall performance. Consequently, different configurations of ejector refrigeration system have been developed for both *heat-driven and compressor-driven* setups.

Received: October 9, 2014
Accepted: January 15, 2015

The purpose of the ejector in the compressor-driven ejector refrigeration cycle is to improve its coefficient of performance (COP) by minimizing the throttling losses caused by the conventional expansion devices. These throttling losses reduce the refrigerating effect of the system, thus also reducing its efficiency and COP.

Figure 1 shows the standard vapor-compression cycle (VCC) and the compressor-driven ejector refrigeration cycle (CDERC) on a P-h diagram. In the standard VCC, the refrigerant flow is point 8, 2b, 3, 11 and 8. Meanwhile, the CDERC has two refrigerant flows: the primary and the secondary flow. The primary flow is circulated by the compressor through condenser, ejector, and separator (point 1, 2, 3, 4, 10, 5 and 1); while the secondary flow circulates in the expansion device, evaporator, ejector, and separator (point 6, 7, 8, 9, 10, 5, and 6) [1].

In the CDERC, the refrigerant at its saturated vapor state (state 1) enters the compressor and is then compressed, increasing its pressure to state 2. The compressed fluid enters the condenser which results in a temperature drop (state 3). The refrigerant enters the ejector as the primary fluid (state 4), where it draws in vapor from the evaporator (state 9). It is then diffused in the diffuser where it recovers pressure (state 5). At the vapor-liquid separator, the refrigerant is separated into two: saturated vapor, which returns to the compressor (state 1), and saturated liquid, which enters the expansion device (state 6). The pressure drops as the fluid exits the expansion device (state 7), and the refrigerant enters the evaporator. It then turns into saturated vapor (state 8) and returns to the ejector as the secondary fluid (state 9).

As shown in Figure 1, the CDERC has a higher suction pressure compared to the standard VCC. Thus, the compressor work for the CDERC is lower than of the standard cycle.

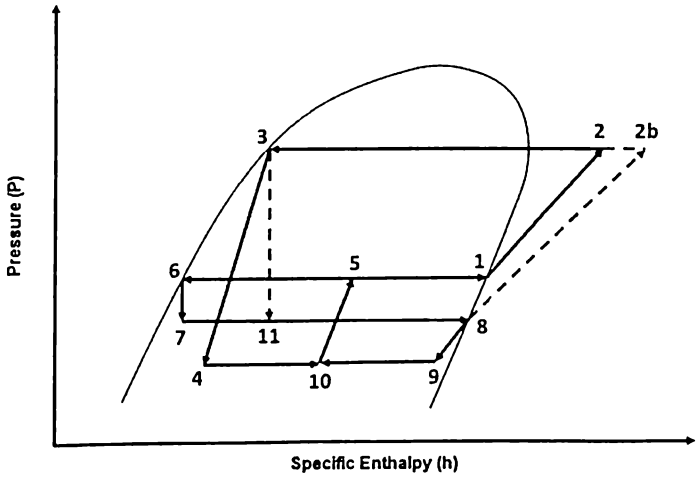

Figure 1. P-h diagram of the CDERC and the standard VCC

Figure 2 and Figure 3 show the schematic diagrams of the CDERC and the standard VCC. The vapor refrigerant in the separator circulates through the compressor and condenser as the primary flow, whereas the liquid refrigerant from the separator circulates through the expansion valve and evaporator as the secondary flow.

The goal of this paper is to produce a model for designing the ejector by specifically determining dimensions that include the nozzle, pre-mixing chamber, mixing chamber and

diffuser. The design is based on the thermodynamic properties of the refrigerant without allowing the ejector to experience shock. Pressure and velocity can be also determined across the length of the ejector together with the thermodynamic values at discreet points. The model will be also used in producing the ejector geometry, with its pressure and velocity profiles, based on desired input parameters for the system.

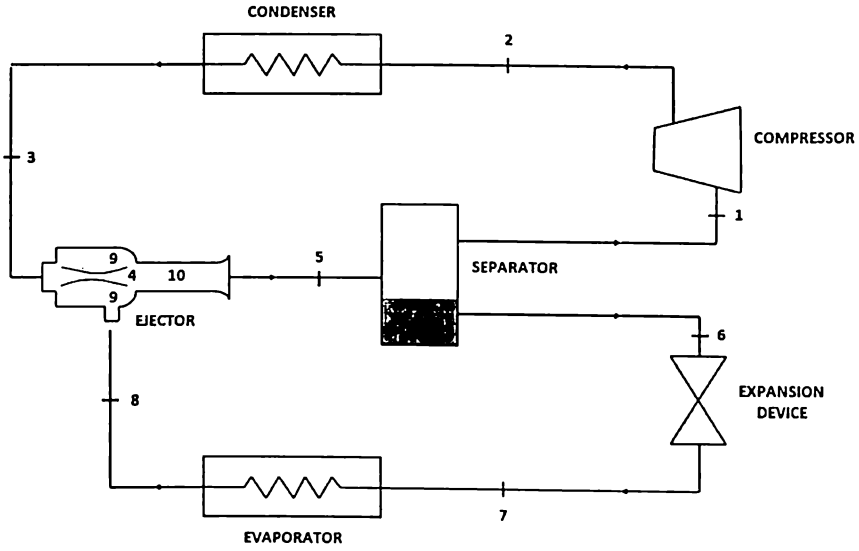

Figure 2. Schematic diagram of the CDERC

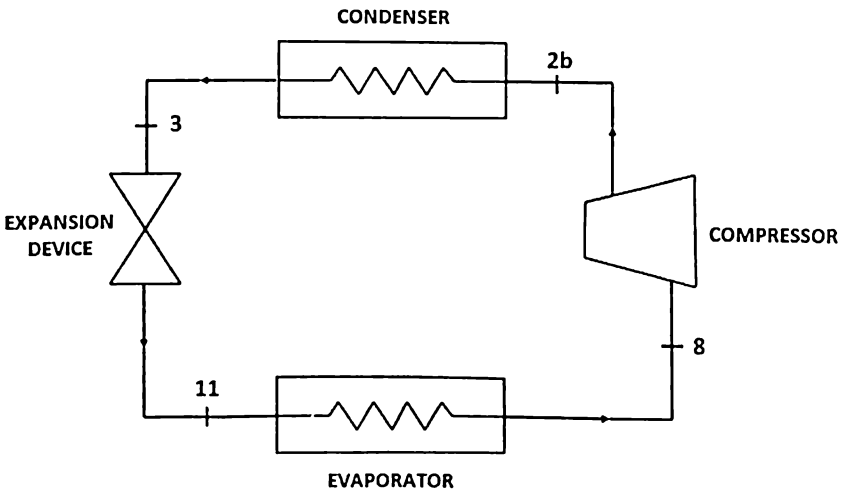

Figure 3. Schematic diagram of the standard VCC

2. THEORY AND METHODOLOGY

2.1. Governing Equations for the Two-Phase Flow

The analysis of two phase flow within the system is assumed to be homogenous, and it is limited to one-dimensional flow [2-3]. The quality of the fluid is integrated in all of the governing equations used.

2.1.1. Conservation of Mass

The fluid is considered to undergo steady flow process in an open system, this means that the mass that flows in must flow out, then

$$\dot{m}_1 = \dot{m}_2 \tag{1}$$

$$\frac{u_1 A_1}{v_1} = \frac{u_2 A_2}{v_2} \tag{2}$$

$$\frac{u_1 A_1}{v_{f1} + x_1 v_{fg1}} = \frac{u_2 A_2}{v_{f2} + x_2 v_{fg2}} \tag{3}$$

where,

$\dot{m}$ = mass flow rate
u = velocity of the fluid
A = cross-sectional area of the channel
v = specific volume of the fluid
x = quality of the fluid

2.1.2. Conservation of Energy

The assumption is that the flow is adiabatic and the effect of gravity is negligible because the ejector is placed horizontally. Then the conservation of energy equation in quality form (since the fluid is in two phase flow) will be

$$\left(h_{f1} + x_1 h_{fg1}\right) + \frac{u_1^2}{2} = \left(h_{f2} + x_2 h_{fg2}\right) + \frac{u_2^2}{2} \tag{4}$$

where,

h = enthalpy of the fluid

2.1.3. Conservation of Momentum

The momentum equation to be used is based on the equation derived by Berana [3] which incorporates the friction factor f, based on the fluid's Reynold's number, *Re*.

$$-v\frac{dP}{dz} = \frac{d}{dz}\left(\frac{u^2}{2}\right) + 2f\frac{u^2}{D} \tag{5}$$

The Blasius-type friction factor was used in this paper and it is written in the form [4-5]

$$f = CRe^{-n} \tag{6}$$

where,

C = 0.118 (constant coefficient)
n = 0.165 (Blasius index)
Re = $uD/v\mu$

The Reynolds number can be modified to fit two-phase model to be

$$Re = \frac{uD}{\left(v_f + xv_{fg}\right)\left(\mu_f + x\mu_{fg}\right)} \tag{7}$$

2.1.4. Speed of Sound

The speed of sound calculation is based on Berana's formulation of the speed of sound under the two phase region [3]

$$c^2 \approx \left(\frac{\partial P}{\partial \rho}\right) = \frac{-v^2 \dfrac{dP}{dT}}{\dfrac{dv}{dT}} \tag{8}$$

where,

$$\left(\frac{dP}{dT}\right) = \frac{s_g - s_l}{v_g - v_l} \tag{9}$$

is the Clausius-Clapeyron equation, and

$$\frac{dv}{dT} = -\left[x\frac{ds_g}{dT} + (1-x)\frac{ds_l}{dT}\right]\left(\frac{1}{\dfrac{dP}{dT}}\right) + x\frac{dv_g}{dT} + (1-x)\frac{dv_l}{dT} \tag{10}$$

The Mach number which is the ratio of the local speed of the fluid to the corresponding local speed of sound is the one used in the program to show velocity profiles.

2.2. Ejector Parts Numerical Scheme [6]

The parts of the ejector are shown in Figure 4.

2.2.1. Nozzle

The equations for conservation of mass, momentum and energy were used to simulate the changes in properties of the flow and determine the difference in cross-sectional area along the length of the nozzle.

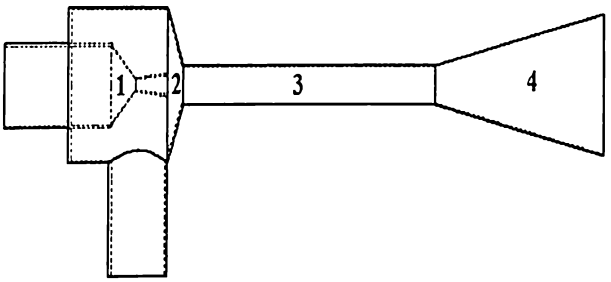

Figure 4. Parts of the ejector: (1) nozzle, (2) pre-mixing section, (3) mixing chamber, (4) diffuser

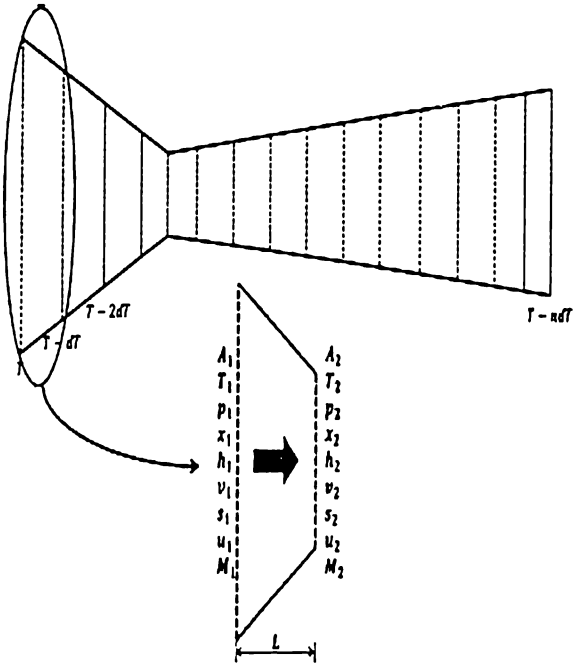

Figure 5. Nozzle diagram with states 1 and 2 and their corresponding thermodynamic values

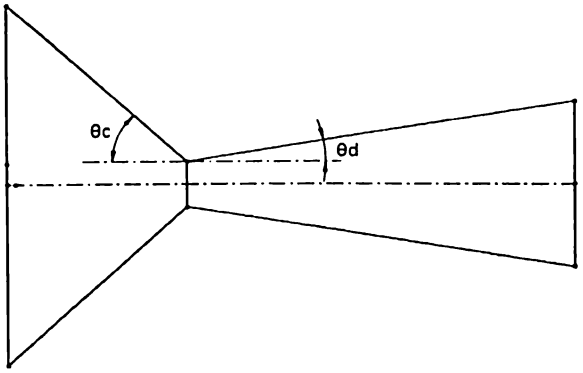

Figure 6. Geometry of the converging-diverging nozzle

Shown in Figure 5 are the thermodynamic values of state 1 (T_1, P_1, h_1, s_1, v_1, u_1, U_1, M_1, *and* D_1) which is the inlet of each discrete section of the nozzle. State 2 (T_2, P_2, h_2, s_2, v_2, u_2, U_2, M_2 and D_2) will be determined using the three governing equations stated below.

For an adiabatic process, the conservation of energy equation can be simplified as

$$-dh = d\left(\frac{u^2}{2}\right) \tag{11}$$

The equations for continuity and conservation of momentum will be the same as that of Eq. (3) and (5). From Eq. (11), we can solve the velocity to be

$$U_2 = \sqrt{2(h_1 - h_2)} \tag{12}$$

The length L of the converging nozzle can be solved using Eq. (13) and the diameter for the converging section from the continuity equation to be Eq. (14).

$$L = \frac{D_1\left(1 - \sqrt{\left(\frac{u_1}{u_2}\right)\left(\frac{v_2}{v_1}\right)}\right)}{2tan\theta_c} \tag{13}$$

$$D_2 = D_1 - 2Ltan\theta_c \tag{14}$$

The next iteration will be computed by testing convergence with the combination of the energy and the momentum equation

$$dh = vdP + 2f\frac{u^2}{D}dz \tag{15}$$

The iteration will continue until the Mach number of the fluid becomes 1. This means that the iteration finally reaches the throat of the converging-diverging nozzle. A different but similar set of equations is used for the diverging part of the nozzle

$$L = \frac{D_1\left(-1+\sqrt{\left(\frac{u_1}{u_2}\right)\left(\frac{v_2}{v_1}\right)}\right)}{2tan\theta_d} \tag{16}$$

$$D_2 = D_1 + 2Ltan\theta_d \tag{17}$$

Eq. (15) is used as the convergence criterion for the iteration.

2.2.2. Pre-Mixing Section

The primary fluid is the one that passes through the converging-diverging nozzle for it to achieve a high velocity and relatively lower pressure. Since the velocity of the secondary fluid (the one entrained from the evaporator) is subsonic, there will be a sheer layer/boundary to overcome before they will be fully mixed. The condition for mixing is for the two fluids to achieve the same pressure and for the secondary flow to achieve Mach 1.

The diverging stream from the primary flow should be opposed by a converging stream from the secondary flow; this will also accelerate the secondary fluid to achieve sonic flow [3]. The way of solving for this section is the same as that of the converging part of the nozzle; thus, Eq. (1) to (15) are applicable. The equations for length and diameter of the converging pre-mixing section will be generalized as

$$L = \frac{D_1\left(1-\sqrt{\left(\frac{u_1}{u_2}\right)\left(\frac{v_2}{v_1}\right)}\right)}{2tan\theta_{se}} \tag{18}$$

$$D_2 = D_1 - 2Ltan\theta_{se} \tag{19}$$

The iteration will stop if the two fluid flows have the same pressure and if the secondary flow achieves a sonic velocity. Hence, it is assumed that the two fluids are fully mixed and Eq. (15) is still used as the convergence criterion for the iteration.

2.2.3. Pre-Mixing Section

For the mixing section, the assumption is that the system is not allowed to experience shock; therefore, a good choice from ASHRAE [7] and EDSU [8] is needed. For this paper, it is assumed that

$$L_m = 3D_m \tag{20}$$

2.2.4. Diffuser

The completely mixed fluid at the end of the mixing section will now flow through the diffuser, shown in Figure 7, where its pressure will be elevated but should not reach the superheated state.

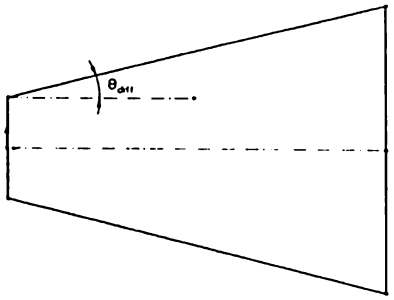

Figure 7. Geometry of the converging-diverging nozzle

The velocity of the fluid will decrease throughout the end of the diffuser. The angle range for the diffuser is also based from ASHRAE [7] and EDSU [8]. For the diffuser, the equations used for the previous sections can also be used. By applying the conservation of mass and the geometry equations, the length and diameter can be computed as:

$$L = \frac{D_1\left(-1+\sqrt{\left(\frac{u_1}{u_2}\right)\left(\frac{v_2}{v_1}\right)}\right)}{2tan\theta_{diff}} \tag{21}$$

$$D_2 = D_1 + 2Ltan\theta_{diff} \tag{22}$$

Eq. (15) is used as the convergence criterion for every discrete point. One of the stopping conditions for the diffuser is to achieve a velocity less than 20 m/s based on ASHRAE, but in the program we force the velocity to achieve 0 m/s to use all the kinetic energy in the fluid. The outlet quality of the fluid at the diffuser should also be checked. It should follow the condition:

$$x_5 = \frac{1}{1+\omega} \tag{20}$$

where, ω is the entrainment ratio.

3. LIMITATIONS AND PROBLEMS ENCOUNTERED

The program produced for this paper is used to design an ejector as part of a compressor-driven refrigeration system with an evaporating temperature of -5°C, condensing temperature of 40°C, and evaporator mass flow rate of 0.2 kg/s. The input parameters are varied for each of the eight refrigerants consisting of ammonia, water, R22, R134a, R1234yf, R245fa, and propane.

The program was compiled and executed using MARUO [9] software to call values from REFPROP [10] by using functions made using FORTRAN and coded using the C programming language. The program follows the equations presented in Section 2.

The output of the program such as the ejector radius/diameter, pressure, and velocity/Mach number are tabulated and plotted using MS Excel. The first program which only operate under the vapor dome, works for the entire refrigerant list except for water and CO_2. The ejector system however was impossible to work with water as its refrigerant because the expansion and compression processes hits the triple point of water. For the case of carbon dioxide, it is transcritical across the ejector, meaning at some point on either compression or expansion, it will bypass the vapor dome and be in the single phase region. The governing equations and iterative equations discussed above will not work outside of the vapor dome; therefore, an established number of equations working in the single phase region was implemented.

4. RESULTS AND DISCUSSION

The program for the compressor-driven refrigeration ejector was simulated using different refrigerants with the same input temperature for the evaporator and condenser which are -5°C and 30°C, respectively, and the same evaporator mass flow rate of 0.2 kg/s. The data produced by the program was post-processed using MS Excel and the geometry together with the pressure and velocity profile for the entire length of the ejector was plotted and presented as graphs. It can be easily seen in the graphs that across the ejector profile, the pressure and velocity follow the desired trend for the flow inside the ejector.

4.1. Resulting Graphs for a Compressor-Driven Ejector System Using Ammonia as Refrigerant

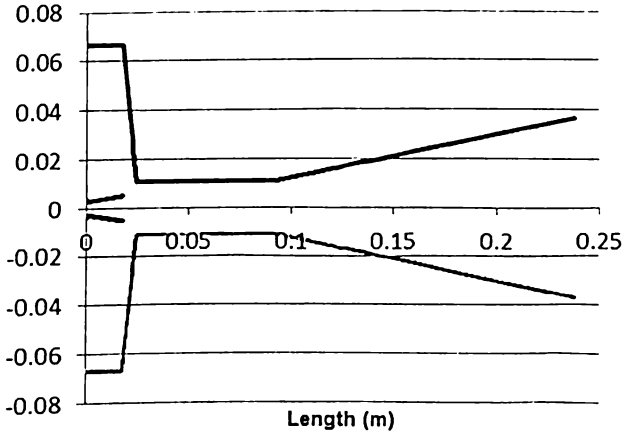

Figure 8. Ejector profile for ammonia

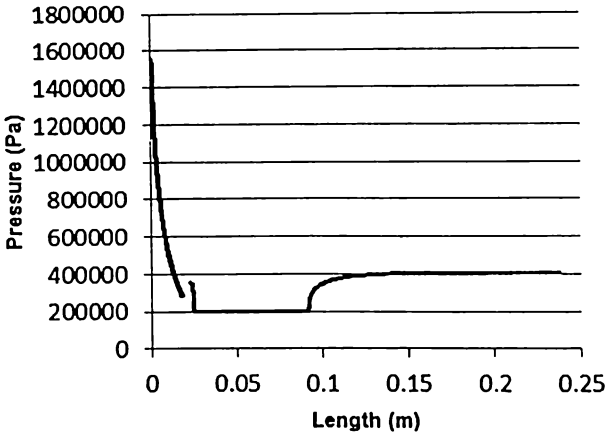

Figure 9. Pressure profile for ammonia

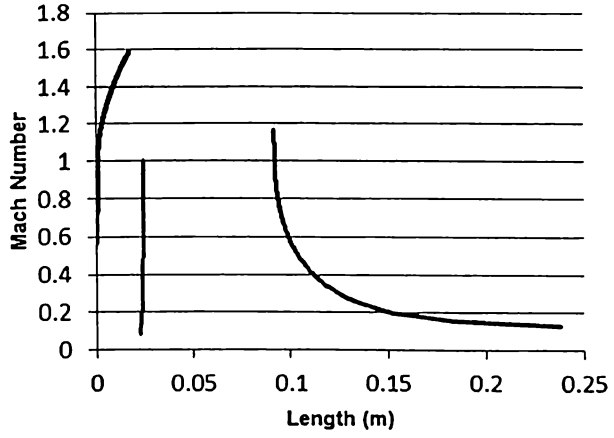

Figure 10. Mach number profile for ammonia

4.2. Resulting Graphs for a Compressor-Driven Ejector System Using R22 as Refrigerant

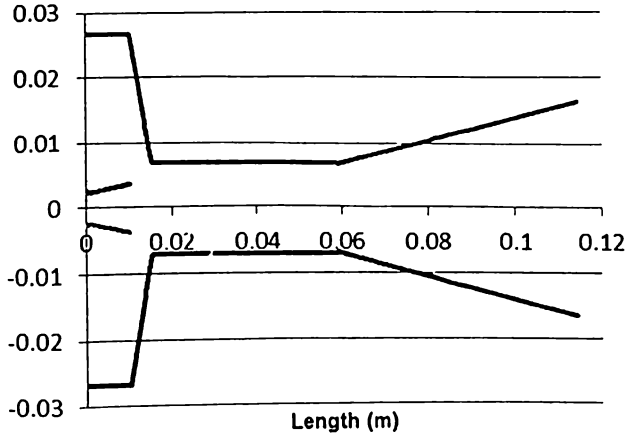

Figure 11. Ejector profile for R22

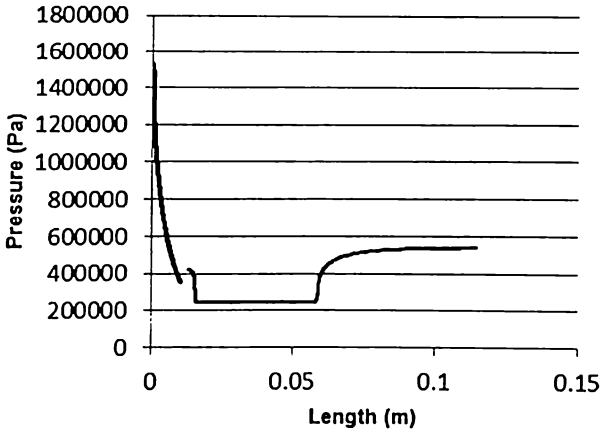

Figure 12. Pressure profile for R22

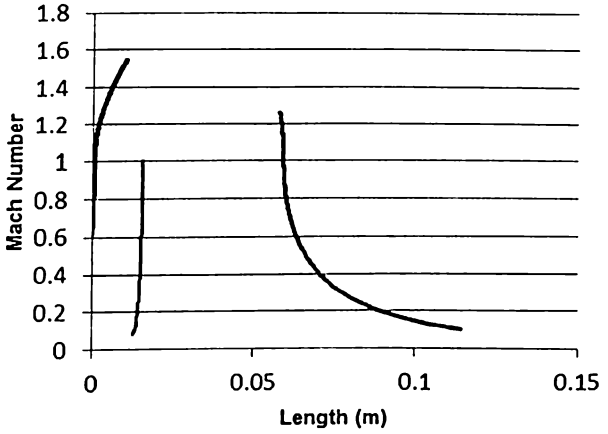

Figure 13. Mach number profile for R22

4.3. Resulting Graphs for a Compressor-Driven Ejector System Using R134a as Refrigerant

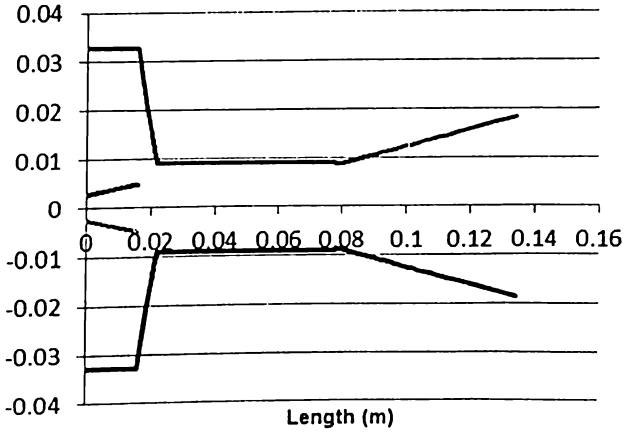

Figure 14. Ejector profile for R134a

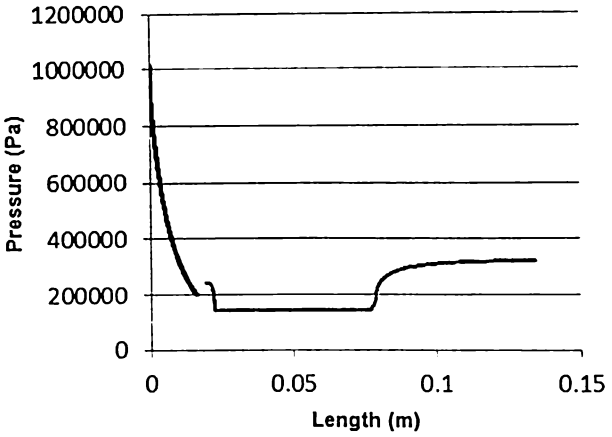

Figure 15. Pressure profile for R134a

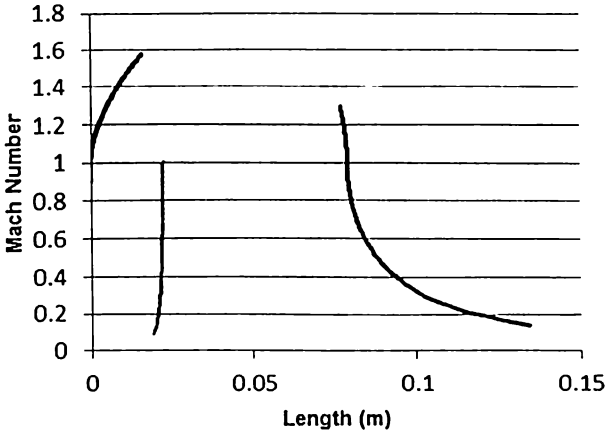

Figure 16. Mach number profile for R134a

4.4. Resulting Graphs for a Compressor-Driven Ejector System Using R1234yf as Refrigerant

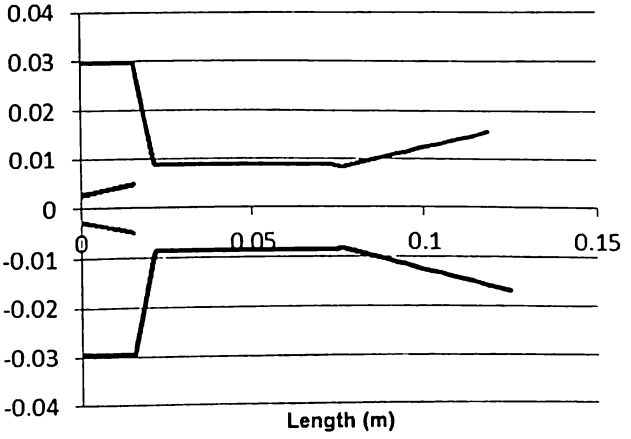

Figure 17. Ejector profile for R1234yf

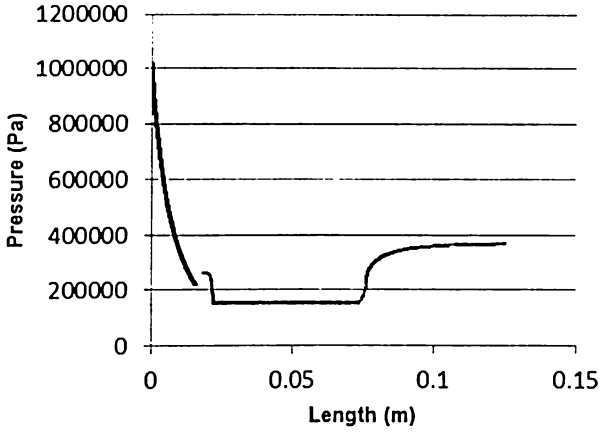

Figure 18. Pressure profile for R1234yf

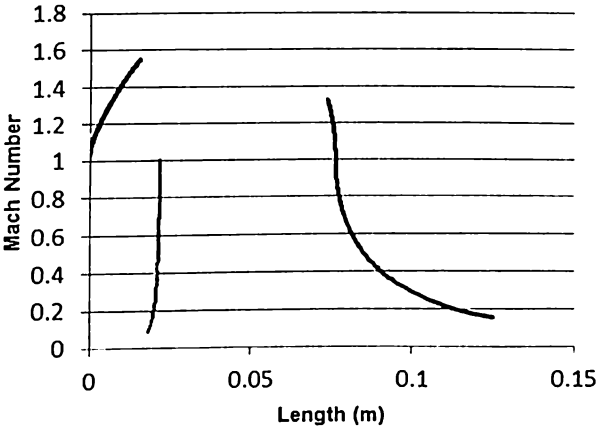

Figure 19. Mach number profile for R1234yf

4.5. Resulting Graphs for a Compressor-Driven Ejector System Using R245fa as Refrigerant

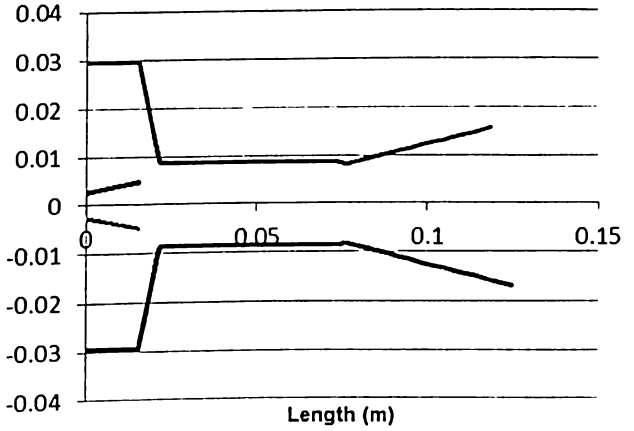

Figure 20. Ejector profile for R245fa

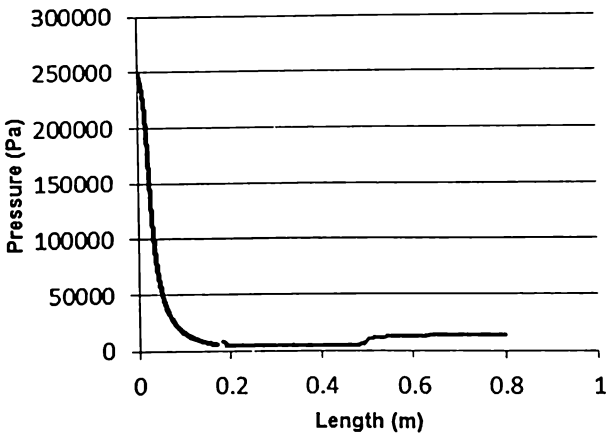

Figure 21. Pressure profile for R245fa

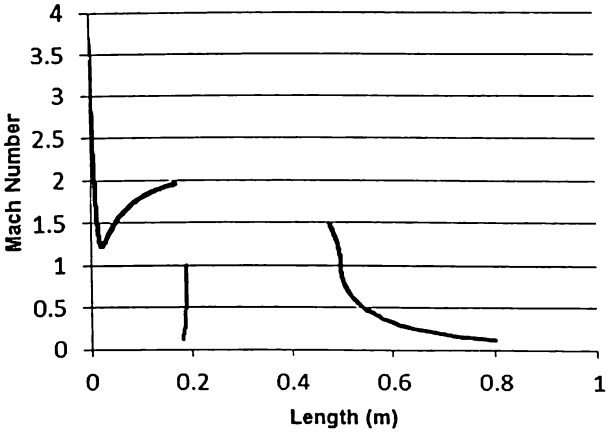

Figure 22. Mach number profile for R245fa

4.6. Resulting Graphs for a Compressor-Driven Ejector System Using Propane as Refrigerant

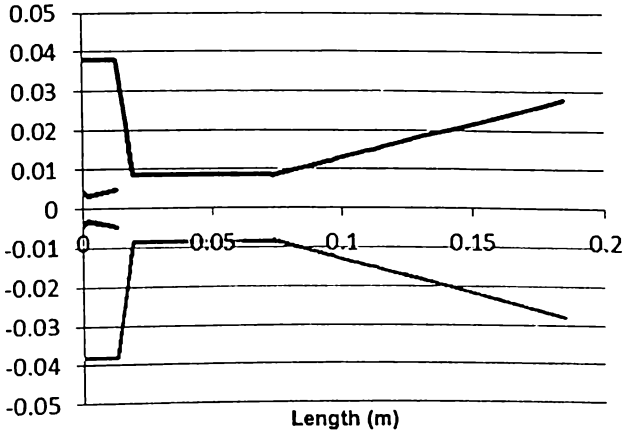

Figure 23. Ejector profile for propane

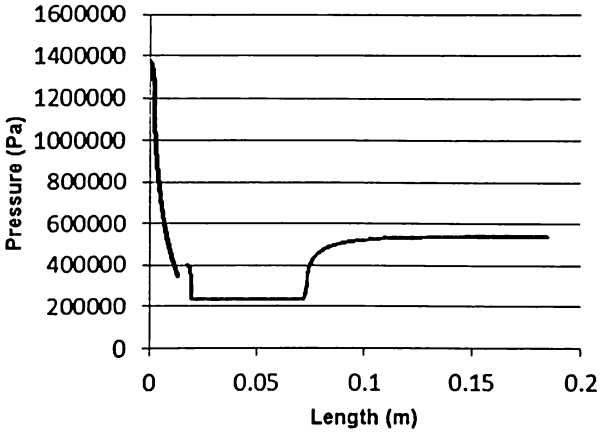

Figure 24. Pressure profile for propane

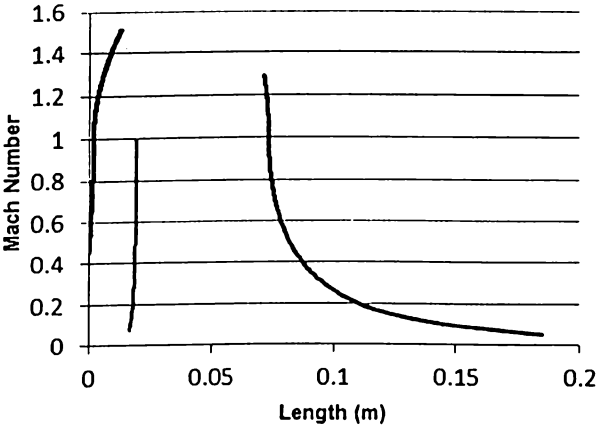

Figure 25. Mach number profile for propane

4.7. Comparison among the Refrigerants

Another goal of the study is to observe the performance of the six refrigerants when used in a compressor-driven ejector refrigeration system. Initially, the following input parameters are the same for all refrigerants: evaporating temperature, condensing temperature and evaporator mass flow rate.

The entrainment ratio is varied until it satisfies the criterion set by Eq. (23).

As seen in Table 1, R245fa has a different evaporating temperature compared to other refrigerants. This refrigerant is not suitable for given set-up wherein the evaporating temperature is at -5°C. It requires a lower temperature.

The following separator temperatures are also obtained from the program: ammonia (-1.4°C), R22 (2.5°C), R134a (2.8°C), R1234yf (-4.7°C), R245fa (-26.3°C), and propane (4.3°C).

Entrainment ratio (ω) is defined as the ratio of the amount of secondary fluid to the amount of primary fluid. For CDERC, it is expressed as

$$COP = \frac{Refrigerating\ Capacity}{Compressor\ Power} = \frac{\dot{Q}_{evap}}{\dot{W}_{comp}} \tag{25}$$

Table 1. Input parameters of each refrigerant

Refrigerant	Evaporator Temperature (°C)	Condenser Temperature (°C)	Evaporator Mass Flow Rate (kg/s)	Entrainment Ratio, ω
Ammonia	-5	40	0.2	0.85
R22	-5	40	0.2	0.78
R134a	-5	40	0.2	0.75
R1234yf	-5	40	0.2	0.72
R245fa	-35	40	0.2	0.63
Propane	-5	40	0.2	0.76

Table 2. Performance of each refrigerant for the two systems

Refrigerant	Refrigerating Effect (kJ/kg)		Specific Compressor Work (kJ/kg)		COP		COP Improvement
	VCC	CDERC	VCC	CDERC	VCC	CDERC	
Ammonia	1066.01	1263.12	215.5	193.4	4.95	5.55	12%
R22	153.51	200.22	32.36	25.91	4.74	6.03	27%
R134a	139.25	191.89	29.75	23.78	4.68	6.05	29%
R1234yf	105.12	153.91	23.89	18.05	4.40	6.14	40%
R245fa	126.63	212.16	56.89	48.45	2.23	2.76	24%
Propane	262.12	358.48	56.97	43.46	4.60	6.27	36%

Using Eq. (25) and Tables 1-2, the COP for a standard VCC and for CDERC is obtained.

$$COP_{VCC} = \frac{\dot{m}_{evap}(h_8 - h_{11})}{\dot{m}_{cond}(h_{2b} - h_8)} = \frac{(h_8 - h_{11})}{(h_{2b} - h_8)} \tag{26}$$

$$COP_{CDERC} = \frac{\dot{m}_{evap}(h_8 - h_7)}{\dot{m}_{comp}(h_2 - h_1)} = \omega\frac{(h_8 - h_7)}{(h_2 - h_1)} \tag{27}$$

For the VCC the mass flow rates in the evaporator and in the condenser are the same. Thus, the COP of a standard VCC is also expressed in the ratio of the enthalpy differences of the two said heat exchangers.

Using Eq. (26) and (27), the COP of each refrigerant for both the standard VCC and CDERC is calculated. Table 2 shows the summary of the refrigerating effect, specific compressor work, and COP of each system for different fluids.

All fluids show that the system is improved when an ejector is used. However, R1234yf is not applicable for an ideal compressor-driven ejector refrigeration system. The compression work of the system is in the two-phase fluid which is not advisable because this can harm the compressor. The evaporating temperature of R245fa is lowered to avoid the same problem encountered in R1234yf which is compression work in the two-phase region.

5. CONCLUSIONS AND RECOMMENDATIONS

The model can determine the ejector profile given the condensing and evaporating temperature, evaporator mass flow rate, and entrainment ratio. It is shown in all refrigerants used in the study that the standard vapor compression cycle is improved by using a compressor-driven ejector. However, it is observed that R1234yf is not suitable for an ideal CDERC given the initial conditions.

One of the parameters that can improve the performance of the ejector is the entrainment ratio. Increasing the mass entrainment ratio will reduce compressor mass flow rate for a given cooling capacity. However, the entrainment ratio cannot be increased as high as possible. This can cause the primary flow to be weak.

A good area for study is choosing the best refrigerant given certain parameters like refrigerating capacity, and operating temperatures of the condenser and evaporator. This will further optimize the compressor-driven ejector refrigerating system. Another area of study is using an internal heat exchanger for CDERC. This could improve the performance of the system using refrigerants like R1234yf and R245fa.

6. REFERENCES

1. Sumeru, K., Nasution, H., Ani, F. N., A Review on Two-Phase Ejector as an Expansion Device in Vapor Compression Refrigeration Cycle, Renewable and Sustainable Energy Reviews, 4927-4937 (2012).
2. Eames, I. W., Aphornratana, S., Da-Wen Sun, The jet-pump cycle-a low cost refrigerator option powered by waste heat, Heat Recovery systems & CHP, vol. 15, no. 8, pp.711-721 (1995).
3. Berana, M.S., Characteristics and shock waves of supersonic two-phase flow of CO2 through converging-diverging nozzles, Doctoral Dissertation, Toyohashi University of Technology, Toyohashi, Aichi, Japan (2009).
4. Bermido, E. T., Ejector design for powerplant application, Master's Thesis, University of the Philippines Diliman, Quezon City, Philippines (2012).
5. Joseph, D.D., Yang, B.H. Friction Factor Correlations for Laminar, Transition and Turbulent Flow in Smooth Pipes. Physica D 239 (2010) 1318-1328.

6. Espeña, G. D., Berana, M. S., Ejector Modeling for Heat-Driven Ejector Refrigeration Systems, Proceedings of the 8th International Conference on Multiphase Flow, May 2013.
7. ASHRAE, 1979. Steam-Jet Refrigeration Equipment, Equipment Handbook, vol.13, pp. 13.1-13.6.
8. ESDU, 1986. Ejectors and Jet Pumps, Design for Steam Driven Flow, Engineering Science Data item 86030, Engineering Science Data Unit, London.
9. Saitou Kikaku, Maruo Editor, Version 7.07 (2007).
10. Lemmon, E. W., Huber, M. L., McLinden, M. O., NIST Standard Reference Database 23: Reference Fluid Thermodynamic and Transport Properties - REFPROP, Version 8.0, National Institute of Standards and Technology (2007).